Salt Dependence of Calicheamicin−DNA Site-Specific Interactions

Girija Krishnamurthy,‡ Michael D. Brenowitz,§ and George A. Ellestad*,‡

Natural Products Research Section, American Cyanamid Co. Medical Research Division, Lederle Laboratories, Pearl River, New York 10965, and Department of Biochemistry, Albert Einstein College of Medicine, Bronx, New York 10461

Received June 8, 1994; Revised Manuscript Received August 30, 1994⊗

ABSTRACT: Calicheamicin γ_1^I site-specifically binds and cleaves three closely spaced tetranucleotide sequences embedded in an AT-rich region of a 142 base pair DNA restriction fragment. Cleavage is observed predominantly at the TCCT, TTGT, and ATCT sequences, of which TCCT is the primary cleavage site. The Gibbs free energies required to bind calicheamicin to these sequences within the DNA restriction fragment have been determined as a function of NaCl concentration at pH 8.1 and 0 °C and at pH 7.5 and 23 and 0 °C. Between 150 mM and 1 M NaCl, calicheamicin binding to all three sequences is insensitive to salt. The insensitivity of calicheamicin binding to salt continues to 50 mM NaCl for the TTGT and ATCT sequences; the ΔG values for calicheamicin binding to these sequences are on the order of −7.8 to −7.9 kcal mol^{-1} over the entire range of NaCl concentrations studied. However, between 150 and 125 mM NaCl, the TCCT sequence displays a sharp transition in the ΔG of calicheamicin binding from −7.6 to −8.9 kcal mol^{-1}. Below 125 mM NaCl, the ΔG values for calicheamicin binding to the TCCT sequence again are invariant. An analysis of the data in terms of polyelectrolyte theory suggests that counterion release from DNA does not contribute significantly to the energetics of the association and that the association of calicheamicin with specific DNA sequences is dominated by nonionic rather than electrostatic forces. Our results further suggest that some calicheamicin binding/cleavage sites are dependent on flanking sequences.

Calicheamicin γ_1^I (**1**) (Lee et al., 1987a,b, 1992), along with esperamicin A_1 (**2**) (Golik et al., 1987a,b), is a member of the enediyne class of DNA-cleaving agents. Its mechanism of antitumor activity is related to its reactivity with DNA. Calicheamicin γ_1^I is unique among the enediynes, in that it exhibits remarkable DNA binding and cleavage specificity for a molecule of only 1367 Da. This agent binds and cleaves primarily homopyrimidine/homopurine regions of duplex DNA sequences, such as TCCT/AGGA, CTCT/GAGA (Zein et al., 1988, 1989) and TTTT/AAAA (Walker et al., 1992). Calicheamicin has been shown to produce bistranded DNA damage to the virtual exclusion of DNA single-stranded lesions. Furthermore, the majority of bistranded lesions consist of abasic sites opposite direct strand breaks (Dedon et al., 1993). On the basis of competition studies with DNA minor groove binders such as netropsin, the Lederle group inferred that calicheamicin interacts in the minor groove rather than the major groove. Atom-transfer experiments have shown that the minor groove DNA binding orientation is unidirectional, with the aglycon aligned toward the 5′-end of the pyrimidine strand while the oligosaccharide binds toward the 3′-side of the pyrmidine-containing strand (DeVoss et al., 1990; Hangeland et al., 1992). Footprinting experiments with calicheamicin ϵ have confirmed these results (Mah et al., 1994a). In addition, they have demonstrated that binding and cleavage sequences are essentially identical. This is in accord with the thermodynamics of the association to DNA being the determining factor in the observed specificity. Interestingly, the Townsend group showed that calicheamicin γ_1^I cleavage of free DNA known to form nucleosomes shows a periodic pattern that correlates to structural periodicities found in the DNA. Thus, they proposed that calicheamicin recognizes and cleaves DNA sequences with a narrow minor groove, sequences that contain structural discontinuities deviating from regular B-form DNA, and those regions with a propensity for drug-induced helix deformation (Mah et al., 1994b).

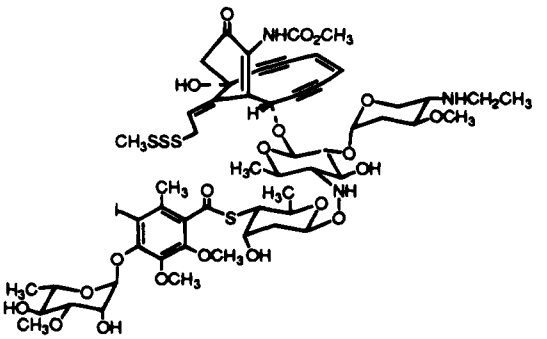

1 Calicheamicin γ_1^I

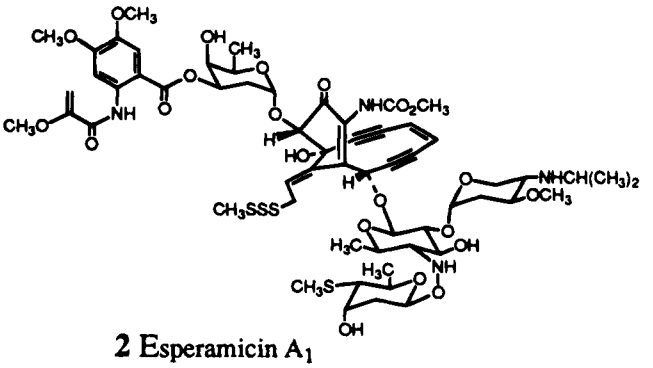

2 Esperamicin A_1

‡ Lederle Laboratories.

§ Albert Einstein College of Medicine.

⊗ Abstract published in *Advance ACS Abstracts,* December 15, 1994.

0006-2960/95/0434-1001$09.00/0

Direct evidence for calicheamicin-induced conformational change in the DNA has been obtained from NMR studies (Walker et al., 1993, 1994). Kahne and co-workers proposed that the drug-induced conformational change in the DNA is the primary determinant for the observed sequence-specific recognition. Specifically, these researchers observed deformation at the 5′-C and 3′-G of an ACCT/TGGA site, with expansion of the minor groove to accommodate the drug.

Recently, we used circular dichroism (CD) spectroscopy to probe calicheamicin-induced conformational changes in a 12-mer containing a preferred TCCT/AGGA recognition sequence (Krishnamurthy et al., 1994). These studies showed that calicheamicin induces an optically detectable conformational change in B-form DNA and that the altered form was reminiscent of alcohol-induced dehydrated DNA structures. This is consistent with the earlier suggestion, based upon temperature-dependent binding studies, that calicheamicin−DNA minor groove association is facilitated by the displacement of water molecules bound to the apolar surfaces of the drug and solvation layers of the DNA (Ding & Ellestad, 1992). Displacement of condensed sodium ions by the positively charged amino sugar (E) and drug-induced conformational changes coupled with altered hydration states of the DNA could also contribute entropically to calicheamicin binding (Eftink et al., 1983).

On the basis of a comparison of disulfide exchange chemistry with calicheamicin γ_1^I and the neutral *N*-acetyl derivative with various thiols in acetonitrile (Ellestad et al., 1989), the ethylamino sugar was originally suggested to play a catalytic role in the reductive cleavage of the allylic trisulfide grouping (Zein et al., 1989). Subsequent kinetic studies specifically designed to examine this question have shown that the amino sugar does not offer any catalytic advantage, at least in an aqueous environment (Chatterjee et al., 1993; Cramer & Townsend, 1991). Instead, the Townsend group proposed that the amino sugar is solely involved in nonspecific Coulombic attraction with the polyanionic DNA backbone. However, the role of the amino sugar in DNA binding and cleavage remains the subject of some debate (Myers et al., 1994). Our current efforts reported here have focused on determining the potential role of electrostatic interactions and their contribution to the overall binding energy. Specifically, we are interested in determining whether counterion release (Record et al., 1978; Wilson & Tanious, 1994) and ion pair formation between the positively charged amino group and the oppositely charged DNA phosphate backbone significantly contribute to the tightness of the interaction. Association constants for protein−DNA interactions and several cationic DNA-binding ligands, such as daunomycin, netropsin, and the steroidal diamine irehdiamine, are influenced by changes in ionic strength (Chaires et al., 1982). These salt effects are related to counterion release and stabilization of the ligand−DNA complex by electrostatic interactions.

As a first step toward understanding the role of the amino sugar in DNA binding interactions, we have determined the binding constants for specific sequences in a 142 base pair fragment as a function of ionic strength. For the determination of binding constants, we have used a site-specific cleavage method based upon the principles of a quantitative footprinting assay developed by Ackers and co-workers (Brenowitz et al., 1986a,b; Senear et al., 1986) and a more recent quantitative affinity cleavage method of Dervan's group (Singleton & Dervan, 1992a,b; Colocci et al., 1993). We report here (i) the sequence specificity of calicheamicin γ_1^I-mediated DNA cleavage in a pBR322 DNA fragment and (ii) binding constants for TCCT, ATCT, and TTGT sequences and their salt dependencies. The results suggest that calicheamicin γ_1^I interaction with DNA is not accompanied by sodium ion release, at least in the sense of the counterion condensation theory. Therefore, Coulombic attraction between the positively charged amino group and the negatively charged sugar phosphate backbone does not significantly contribute to the overall energetics of calicheamicin−DNA sequence-specific association.

MATERIALS AND METHODS

Preparation of Radiolabeled DNA Fragments. pBR322 DNA (75 μg) was linearized by digestion with *Hin*dIII (1.5 units/mg) restriction endonuclease. The 5′-ends were dephosphorylated using calf intestinal phosphatase. The 5′-ends were labeled using [γ-^{33}P]ATP and polynucleotide kinase. The end-labeled DNA was then secondarily digested with *Nci*I (1.3 units/mg) and purified on a polyacrylamide gel. The 142 base pair fragment of interest was isolated from the gel by electroelution and purified. Similarly, the 142 base pair 3′-end-labeled DNA fragment was prepared using [α-^{33}P]ATP and Klenow polymerase. Purified DNA was resuspended in 1 mL of 10 mM Tris buffer to yield an estimated DNA stock concentration of ~20 nM and a radiochemical concentration of 4×10^7 cpm/mL.

DNA Cleavage Reactions for Binding Free Energy Determinations. In a typical experiment, a DNA buffer mixture was prepared by combining Tris-HCl buffer with appropriate concentrations of NaCl and 5′-end-labeled DNA (~1 nM). The buffer mixture was allowed to equilibrate in an ice bath for 30 min. The pH of Tris buffer was measured after temperature equilibration. A 10 OD stock solution of poly-(dG−dC)$_2$ was combined with the buffer/labeled DNA mixture. Equal volumes of the DNA/buffer mixture were transferred to 16 microcentrifuge tubes and equilibrated in an ice bath for 30 min. Calicheamicin was freshly prepared as a 1 mM stock solution in ethanol. Working stock solutions of calicheamicin (10×), composing a four-fold concentration range of 50 nM to 100 μM, were prepared by serially diluting the master stock solution into ethanol. Appropriate calicheamicin stock solutions were transferred to the DNA buffer mixture in microcentrifuge tubes. The final ethanol content in the reaction mixture was 10%. The last tube served as control, to which an equivalent volume of ethanol was added. All DNA−calciheamicin solutions were equilibrated for 3 h prior to the initiation of cleavage chemistry. DNA cleavage was initiated by the addition of 2-mercaptoethanol to a final concentration of 1 mM. At the onset of the cleavage reaction, the reaction medium consisted of 90:10 50 mM Tris buffer (pH 8.1)/ethanol, 2 μM poly-(dG−dC) in base pairs, 0.14 μM in base pairs of labeled DNA fragment, 1 mM mercaptoethanol, and appropriate concentrations of calicheamicin and NaCl. The cleavage reaction was quenched after 10 min by the addition of a large excess of calf thymus DNA and 1% SDS. Products from a given cleavage reaction were recovered by precipitation from aqueous ethanol.

DNA Cleavage Reactions for Mapping Experiments. Mapping experiments were conducted in the presence of either calf thymus DNA or poly(dG−dC)$_2$ as carrier. In a typical mapping experiment, either 5′- or 3′-end-labeled DNA

was transferred to a microcentrifuge tube containing Tris-HCl buffer (pH 8.1) and NaCl. Poly(dG−dC)$_2$ was combined with the labeled DNA mixture. Equal volumes of the buffer/DNA mixture were transferred to three microcentrifuge tubes and equilibrated at 0 °C, as indicated earlier. Calicheamicin stock solutions were transferred to two tubes, and the last one served as a control to which an equivalent volume of ethanol was added. The reaction mixture was equilibrated in an ice bath for 3 h, after which 2-mercaptoethanol was added to initiate cleavage. The following were the final concentrations of the reaction components: 90:10 50 mM Tris buffer (pH 8.1)/ethanol; 125 mM NaCl; 2 μM poly(dG−dC)$_2$; 1 nM labeled DNA; 1 mM 2-mercaptoethanol; and either 1 or 10 μM calicheamicin. The cleavage reaction was quenched after 10 min with excess calf thymus DNA. In another mapping experiment, poly(dG−dC)$_2$ DNA was replaced with calf thymus DNA as carrier, with all other reaction conditions remaining identical to the one described earlier. The DNA cleavage products were recovered by ethanol precipitation for further analysis. The recovered DNA was resuspended in water and divided equally between two microcentrifuge tubes. The first sample was lyophilized directly without further treatment. To the second DNA mixture was added putrescine to a final concentration of 100 mM, and the mixture was then heated at 37 °C for 1 h. The reacted DNA was isolated by ethanol precipitation.

Gel Analysis of Cleavage Products. Formamide/bromophenol blue loading solvent (11 μL) was added to the recovered DNA pellet. To facilitate dissolution of DNA in the loading solvent, it was briefly heated to 55 °C. Two microliters of the DNA solution was then transferred to a scintillation vial consisting of 10 mL of a liquid scintillant, and the radioactivity was assayed in the samples. On the basis of the radioactivity assay, volumes corresponding to equal counts were aliquoted and transferred to fresh microcentrifuge tubes. The final loading volume was adjusted to 9 μL using the formamide solvent. The DNA solution was denatured by heating at 90 °C for 2 min and quickly cooling in an ice bath prior to loading on a 7% denaturing polyacrylamide gel. The DNA was electrophoresed at a constant voltage of 1800 V until the bromophenol blue dye migrated to the bottom of the gel. After electrophoresis, the gel was dried and autoradiographed using preflashed Kodak X-OMAT AR film.

Determination of Binding Free Energies. Binding free energies for the interaction of calicheamicin with TCCT sequences in the 142 base pair DNA were determined at a pH of either 7.5 or 8.1. The duration of the cleavage reaction was limited (indicated earlier) to allow detection of the radioactive band at the lowest calicheamicin concentration and to obtain an average of single-hit kinetics (Brenowitz et al., 1986a) at higher concentrations. The approximation was made that free ligand concentration is equivalent to the total concentration. Poly(dG−dC)$_2$ DNA was used as a carrier to avoid spurious DNA cleavage activity, which resulted in irreproducibility of the cleavage intensities. The oligomer cleavage products were resolved and detected using the electrophoretic method described earlier. The electrophoretic bands visualized on the autoradiograms corresponding to calicheamicin cleavage sites were quantitated using a microcomputer-based videodensitometer (Reiner & Brenowitz, 1991). Densitometric analysis was conducted using a microcomputer implementation (M. Brenowitz, P. Reiner, and B. Turner, unpublished computer programs) of the computer software originally described in Brenowitz et al. (1986a,b).

Binding curves were obtained by quantitating the increase in the OD of the bands representing cleavage sites as a function of free calicheamicin concentration. Rectangles were drawn encompassing the bands, and the appropriate local background corrections were implemented automatically by the analysis software. The value of r_i, the relative OD of a cleavage band, was calculated by

$$r_i = \frac{OD_i}{OD_{ref}} \tag{1}$$

where OD_i is the integrated optical density of a band at a given calicheamicin concentration and OD_{ref} is the reference lane optical density (usually the highest calicheamicin). Values for the equilibrium dissociation constant, K_i, were obtained by treating the data as transition curves and fitting the data to

$$r_i = m\bar{Y}_i + b \tag{2}$$

where

$$\bar{Y}_i = \frac{K_i[X]^{n_H}}{1 + K[X]^{n_H}} \tag{3}$$

where $m = 1/(UL - LL)$ and $b = LL/(LL - UL)$, UL and LL are the upper and lower end points, respectively, of the transition curve, n_H is the Hill coefficient, and $\bar{Y}$ is the fractional saturation of the binding site (Brenowitz et al., 1986a). The Gibbs free energy values ($\Delta G_i = -RT \ln K_i$) and the titration end points were estimated using methods of nonlinear least-squares analysis (Johnson & Faunt, 1992) that determine the best-fit parameter values corresponding to a minimum in the variance, using a variation of the Gauss−Newton procedure that searches the parameter space along a vector dependent on the parameter guesses. The nonlinear least-squares method used in the data analysis returned the 65% joint confidence limits for the estimated parameters (Senear & Bolen, 1992; Koblan et al., 1992).

In the affinity cleavage method employed in this work, site loading and overcutting are sources of inaccuracies that require careful analysis. An overcutting artifact would result in a steady decrease in the density of the bands in the plateau region. On the other hand, sufficient data are required at high drug concentrations to ensure that the upper plateau (saturating drug) is reached. The validity of the best-fit parameters and the sensitivity of the confidence limits were carefully analyzed using various truncations of the data for regeneration of the binding isotherms. In all cases where the correlations of the parameters were acceptable, consistent values of the parameters and the confidence limits were obtained. On the basis of detailed analysis, the titration curves comprise very robust data sets.

RESULTS

Sequence Specificity of Calicheamicin Interaction in a DNA Restriction Fragment. The sequence specificity of calicheamicin-mediated DNA cleavage was determined in the *Hin*dIII−*Nci*I 142 base pair restriction fragment from pBR322. Calicheamicin interaction sites were mapped in the presence of carrier DNA: either calf thymus DNA or poly(dG−dC)$_2$ heteropolymer. Calf thymus DNA competes

with the labeled DNA fragment for binding calicheamicin, and since the carrier DNA is in excess, the concentration of unbound calicheamicin is determined by this substrate. Poly-(dG−dC)$_2$ is not a specific substrate for calicheamicin binding and cleavage events. Figure 1A shows the cleavage distribution in the labeled DNA fragments in the presence of either calf thymus DNA (lanes 4−6) or poly(dG−dC)$_2$ (lanes 1−3). All other reaction conditions were identical in the two experimental sets. In both the presence and absence of calf thymus DNA carrier, conversion of the labeled DNA substrate to oligomer products increases with increases in the concentration of calicheamicin (compare lanes 1−3 and 4−6). The distribution of the cleavage products is identical in the presence of calf thymus DNA and poly(dG−dC)$_2$.

Figure 1B is a densitometric trace of the cleavage distribution on the 5′- and 3′-end-labeled strands. The restriction fragment used in this study consists of the preferred TCCT sequence (Zein et al., 1988, 1989) in the top strand (Chart 1). As illustrated in Figure 1, TCCT is a primary cleavage site with cleavages occurring at the 5′-C on the top strand and shifted by three base pairs toward the 3′-end on the complementary strand. Assignment of all cleavage events is based upon coelectrophoresis with Maxam and Gilbert sequence ladders (Maxam & Gilbert, 1980). The results are consistent with previous binding/cleavage studies (Zein et al., 1988). The two other sequences that we assign as major cleavage sites are TTGT and ATCT. The optical densities of these two cleavage bands are roughly equivalent. As shown in Chart 1, the ATCT and TTGT cleavage sites are interspaced with AT-rich sequences.

TCCT and ATCT sequences are located on the top strand, while the TTGT sequence is located on the bottom strand (Chart 1). The ATCT and TTGT sites are spaced 1 base pair apart on complementary strands. These sequences are cleaved at their penultimate 5′-T residues on the pyrimidine strand and staggered by 3 base pairs toward the 3′-end on the complementary strand. The indicated cleavage preference is identical to the TCCT site. Assignment of cleavage at the TTGT site is based upon gel mobility shifts (Zein et al., 1988; Walker et al., 1992) of calicheamicin-treated DNA before and after putrescine treatment to ensure DNA strand scission of abasic sites originating from 4′-hydrogen atom abstraction (Dedon et al., 1993). Another site of interest due to its proximity to the TCCT site is the TCGT tetramer. This site is located 1 base pair away on the 5′-side of the TCCT site. Cleavage at this site is weak compared to that at the TCCT, ATCT, and TTGT sites, even at the highest calicheamicin concentration.

Salt Dependence of Binding Free Energies. For the determination of the free energies of interaction of calicheamicin with TCCT, ATCT, and TTGT sites, we have used cleavage data on the 5′-end-labeled DNA, top strand. Cleavage bands corresponding to the three sites are 5′-C in the TCCT site, 5′-T in the ATCT site, and at the G residue that is removed 3 base pairs from the penultimate 5′-T for the TTGT site (see Figure 1A, left panel). In our gel analysis, cleavage at these underlined nucleotide residues of the three sequences is better resolved in the 5′-end-labeled strand than in the 3′-end-labeled strand. For the determination of free energies of calicheamicin interaction with TCCT, TTGT, and ATCT sequences on the restriction fragment, optical densities were monitored as a function of the increasing concentration of the drug. 5′-End-labeled DNA (<1 nM) was titrated with increasing concentrations of the drug (5 nM to 10 μM). The labeled DNA concentration is small compared to the dissociation constant of the calicheamicin at the TCCT site (Krishnamurthy et al., 1994).

Figure 2 is a gel analysis of the cleavage reaction at 125 mM NaCl as a function of calicheamicin concentration. Optical densities of each of the three bands were determined using two-dimensional densitometric methods. The integrated OD at each site was converted to fractional saturation and plotted as a function of total calicheamicin concentration.

Binding isotherms were generated for the TCCT, TTGT, and ATCT sites, and the free energy was determined using a nonlinear least-squares fitting procedure (Figure 3). It should be noted that the values determined are individual site loading energies that may include contributions from cooperative interactions (Ackers et al., 1983). The best-fit Hill coefficients (n_H) that were determined for each of the binding curves especially the TCCT sequence, are, in general greater than one (data not shown). These values may indicate either cooperative interactions among calicheamicin molecules bound to the specific sites (see below) or the linkage of calicheamicin self-association with DNA binding.

Figures 4 and 5 show the TCCT binding free energies as a function of the logarithm of the NaCl concentration at pH 8.1 and 0 °C. An unusual free energy dependence on salt is observed with tighter binding below 125 mM NaCl and lower binding above 150 mM salt. At salt concentrations greater than 150 mM, the free energy is −7.5 kcal mol^{-1} and is independent of salt. Between 125 and 150 mM NaCl, there is a steep increase of 1.4 kcal in the free energy of interaction with the TCCT site. Below 125 mM NaCl, the binding free energies of −8.9 kcal are again essentially independent of salt.

The relative sharpness of the saturation transition for the 125 mM NaCl TCCT binding isotherm (Figures 3 and 4) is noteworthy. Although we do not have a ready explanation for this effect, it might be due to overcutting at the TCCT site, which is fortuitously counterbalanced by the depletion of available target molecules having no cuts closer to the labeled end. To check for the possible influence of overcutting on the calculation of the binding free energies, the validity of the calculations was analyzed with regenerated binding isotherms using several truncated data sets in which the highest concentration points of the drug were removed (e.g., Figures 2 and 3). In those instances where the correlation of the parameters and confidence limits was acceptable, the binding free energies were influenced only slightly. In the binding isotherms resulting from the 50 and 100 mM NaCl experiments, such a sharp transition near the saturation region was not observed, even though the binding free energies were comparable (Figure 4). These analyses, taken together, suggest that the sharpness of the transitions in these experiments does not significantly influence the calculation of the binding free energies and, therefore, the interpretation of the salt dependence data.

The free energy of calicheamicin binding to the TCCT site as a function of salt at 23 °C and pH 7.5 (Table 1) and at 0 °C and pH 7.5 was also determined. For the 23 °C experiments, the cleavage reaction time was decreased to 5 min, while all other reaction conditions remained identical to those of the 0 °C experiments. The free energy of interaction of calicheamicin with the TCCT site at 23 °C again shifts to tighter binding at the lower salt concentrations. In this instance, however, the transition to tighter binding occurs below 100 mM NaCl. The overall trend for the salt

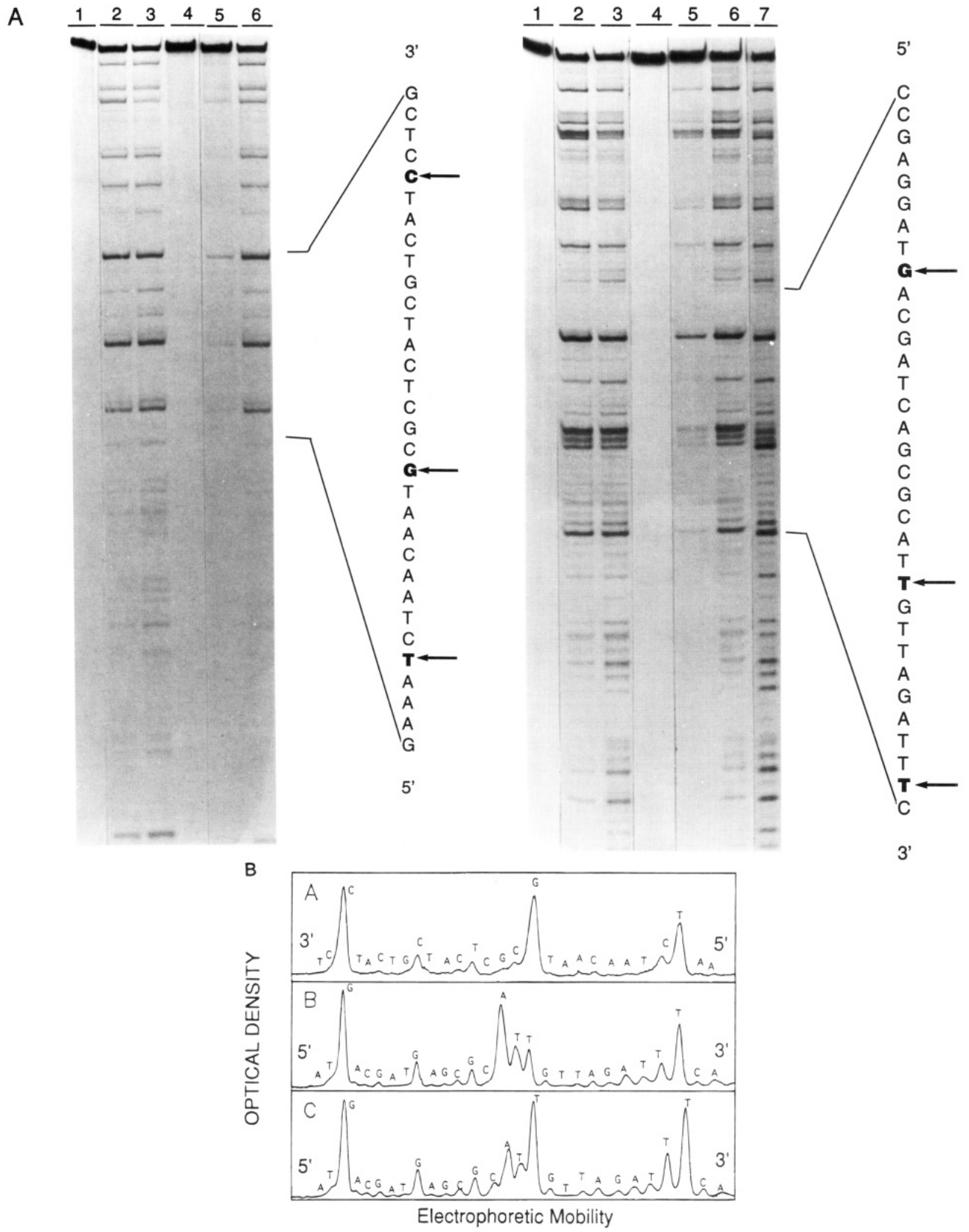

FIGURE 1: Sequence specificity of calicheamicin-mediated DNA cleavage in the *Hin*dIII−*Nci*I restriction fragment. (A) Image of autoradiograms obtained for calicheamicin-mediated DNA cleavage of ^{33}P-labeled products; the left panel is 5′-end-labeled DNA and the right panel is 3′-end-labeled. In both panels, lanes 1−3 and 4−6 are DNA cleavage in the presence of either poly(dG−dC)$_2$ or calf thymus carrier DNA, respectively. All cleavage reactions were carried out in the presence of 125 mM NaCl in Tris buffer at pH 8.1 and 0 °C, according to the procedure described in the Materials and Methods section. The calicheamicin concentration in the cleavage reactions is as follows: lanes 1 and 4, 0; lanes 2 and 5, 1 μM; lanes 3, 6, and 7, 10 μM. Lane 7 indicates the electrophoretic mobility of the cleavage products subsequent to putrescine treatment. The 25 base pair region is identified by the sequence printed on the left and right panels for the 5′- and 3′-end-labeled strands, respectively. Arrows indicate the three major cleavage positions corresponding to the TCCT, TTGT, and ATCT sequences. (B) Densitometric scans of lane 3 in panel A (5′-end-labeled strand) and lanes 3 and 7 in panels B and C (3′-end-labeled strand). The sequence spanning the 28 base pair region (also see Chart 1, sequences between 60 and 90) is indicated on the traces, and the cleavages on the top and bottom strands are aligned along the horizontal axis.

Chart 1

```
          50                  60                  70
5′ A C C G T G T A T G A A A T C T A A C A A T G C G
   T G G C A C A T A C T T T A G A T T G T T A C G C

          80                  90                  100
C T C A T C G T C A T C C T C G G C A C C G T C A C
G A G T A G C A G T A G G A G C C G T G G C A G T G 5′
```

dependence is, however, identical to that reported at pH 8.1 and 0 °C. The free energy of calicheamicin interaction with the TCCT site at 0 °C (pH 7.5) was −7.3 and −7.4 kcal mol^{-1} at 100 and 250 mM NaCl, respectively. In order to determine the effect, if any, of poly(dG−dC)$_2$ carrier DNA on the binding free energies, its concentration was varied to 5- and 10-fold higher relative to labeled DNA at 50 mM NaCl, pH 7.5, and 23 °C and compared to the corresponding experiment at a concentration 14-fold higher than that used in the binding free energy determinations. The binding free energies for the TCCT site were identical for the 5-, 10-, and 14-fold higher carrier DNA concentrations (9.5, 9.4 and 9.6 kcal mol^{-1} respectively; see Table 1). These free energies represent a 2% variation and are identical within the limits of experimental error. Similarly, the binding free energies at TTGT and ATCT sites were also independent of poly(dG−dC)$_2$ at these concentrations.

Binding and cleavage events of the two overlapping sites, TTGT and ATCT, were compared to the TCCT sequence (Figure 3). Figure 3 shows the binding isotherms for the three sites at 125 mM NaCl. At 125 mM salt, calicheamicin binding is weaker at the ATCT and TTGT sites than at the TCCT site. In Figure 5, the free energies for the TTGT and ATCT sites are plotted as a function of NaCl between 50 mM and 1 M. The site binding free energies of the ATCT and TTGT sites are independent of salt. The Gibbs free energies are −7.8 and −7.9 kcal mol^{-1}, respectively, between 50 mM and 1 M NaCl. These binding energies are comparable to those of the TCCT site above 150 mM NaCl.

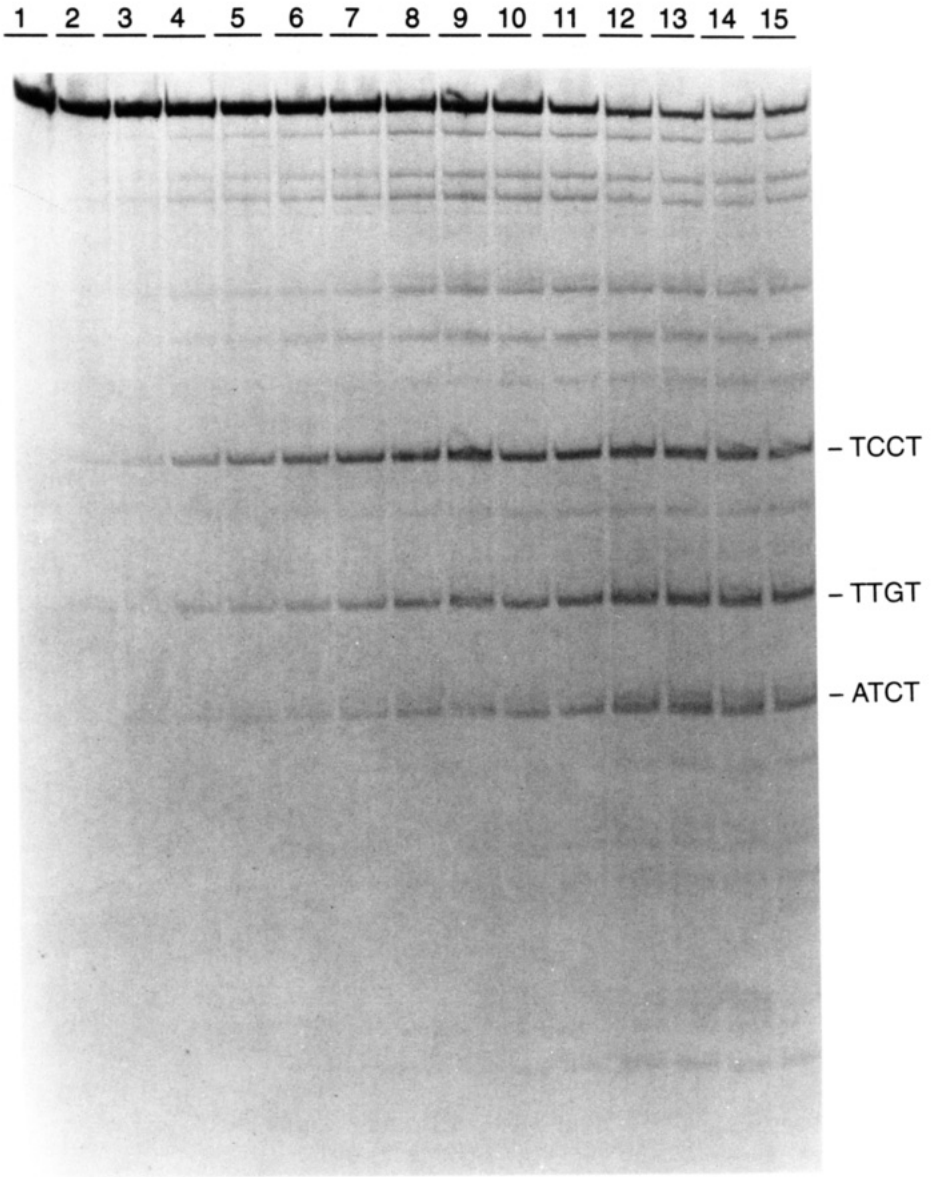

FIGURE 2: Autoradiogram of a high-resolution denaturing polyacrylamide gel used to separate the 5′-end-labeled DNA cleavage products generated by calicheamicin in the presence of poly(dG−dC)$_2$ in 125 mM NaCl/50 mM Tris buffer (pH 8.1) at 0 °C and according to the procedure described in the Materials and Methods section. Lanes 1−15 are site-specific DNA cleavage due to varying calicheamicin concentrations and 1 mM β-mercaptoethanol: 0 calicheamicin (lane 1); 20 nM (lane 2); 40 nM (lane 3); 60 nM (lane 4); 80 nM (lane 5); 100 nM (lane 6); 200 nM (lane 7); 300 nM (lane 8); 400 nM (lane 9); 600 nM (lane 10); 1 μM (lane 11); 2 μM (lane 12); 4 μM (lane 13); 8 μM (lane 14); 10 μM (lane 15). The three cleavage bands are identified by the corresponding tetramer sequences.

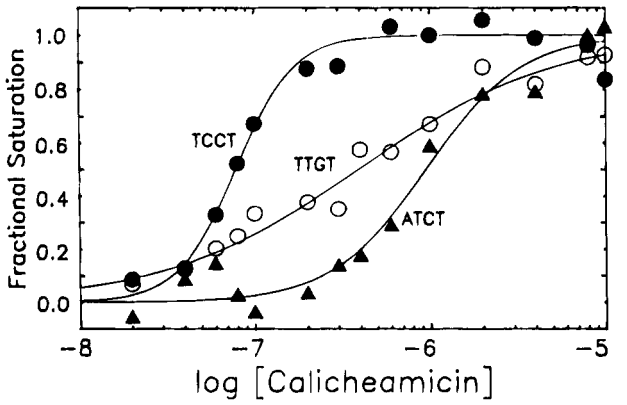

FIGURE 3: Binding isotherms of calicheamicin interacting with TCCT (●), TTGT (○), and ATCT (▲) sequences, whose cleavage data are shown in Figure 2. The symbols represent the fractional saturation data obtained from the relative ODs of the respective cleavage bands in Figure 2. The solid lines connecting the data points are due to nonlinear least-squares fits of the data to the Hill equation.

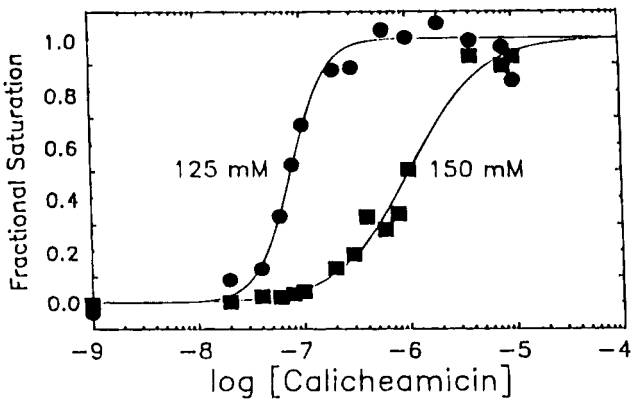

FIGURE 4: Calicheamicin–TCCT site binding isotherms at 125 (●) and 150 mM (■) NaCl (pH 8.1 at 0 °C). The fractional saturation data at 125 mM NaCl were derived from the cleavage data shown in Figure 2. The solid sigmoidal curve in each instance shows the best fit of the data to the Hill equation using nonlinear least-squares analysis.

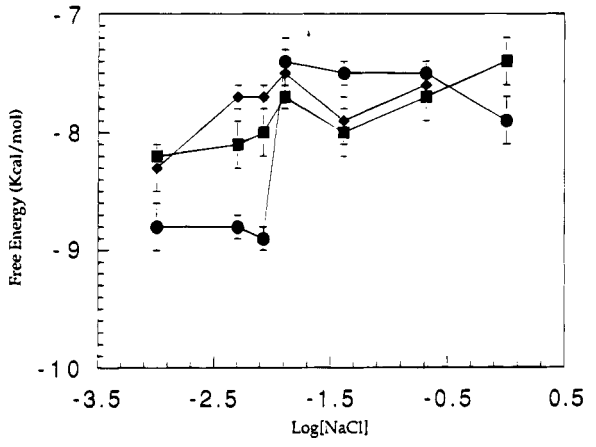

FIGURE 5: Plot of the site binding free energies for calicheamicin interacting with TCCT (●), TTGT (■), and ATCT (◆) as a function of log [NaCl] at pH 8.1 and 0 °C. The error bars represent the 65% confidence interval in the fitted value as described in the Materials and Methods section.

In order to confirm the results obtained by the cleavage method described earlier, we compared the binding free energy for the TCCT site with that obtained using a circular dichroism (CD) method (Krishnamurthy et al., 1994). Therefore, the cleavage experiment was performed using conditions similar to those used in the CD method (100 mM NaCl, pH 7.5, 23 °C), and the binding constant for the TCCT site interaction was determined to be −7.4 kcal mol^{-1}. This value is identical, within experimental error, with that determined by the spectroscopic method.

Table 1: TCCT Site Binding Free Energies as a Function of NaCl Concentration at 23 °C and pH 7.5

NaCl (M)	ΔG^a (kcal mol^{-1})
0.05	−9.6 ± 0.2
0.1	−8.0 ± 0.2
0.25	−8.1 ± 0.2

[a] The errors represent the 65% confidence intervals of the fitted values.

DISCUSSION

An understanding of the physical and chemical properties of calicheamicin and its interaction with DNA is of fundamental importance in evaluating its effectiveness as an anticancer agent. The results of studies of tumor-specific calicheamicin–antibody conjugates in xenograft mice tumors (Lee et al., 1993) have spurred basic studies directed toward the understanding of calicheamicin–DNA association. The observed antitumor effects are likely due to their DNA binding/cleavage properties. It is well established that oligopyrimidine-containing sequences such as TCCT, and more recently TTTT type sequences, are the primary cleavage sites in natural DNA sequences, a conclusion confirmed independently using hydroxyl radical footprinting studies of calicheamicin ϵ (Mah et al., 1994a,b). However, the seemingly simple objective of determining binding constants for calicheamicin interactions with DNA is limited by at least two experimental difficulties. First, unlike many other DNA-binding small molecules, calicheamicin is insoluble in aqueous solutions in the absence of DNA (Myers et al., 1994). A second limiting aspect is the absence of *distinct* spectroscopic features (fluorescence and UV) in calicheamicin. Such spectroscopic methods traditionally have provided valuable information on the DNA binding properties of other small molecules both in natural sequence DNA and in homo- and hetero-DNA polymers.

Recently, we have taken advantage of the changes in the circular dichroism spectrum of B-form DNA due to interaction with calicheamicin (ϵ and γ) to estimate binding constants for the TCCT sequence (Krishnamurthy et al., 1994). The difficulty in the CD method is the absence of a DNA-induced CD for bound calicheamicin. The CD spectrum of calicheamicin, especially in the case of the γ form, significantly overlaps with the DNA CD spectrum, except for the 236 nm wavelength region where its contribution is negligible. Therefore, estimates of binding constants were based upon CD changes at 236 nm as described in our earlier work. In any event, both spectroscopic and physical methods are applicable mainly to DNA models such as oligonucleotide fragments and not to restriction fragments. Binding constant determinations based upon cleavage methods, on the other hand, offer significant advantages in terms of their detection sensitivity. Such a method is especially useful because Townsend and co-workers have recently shown that calicheamicin–DNA site–selective recognition is due solely to a thermodynamic rather than a kinetic selection (C. A. Townsend, personal communication). Here we have used the sensitivity of the affinity cleavage method to estimate

site-specific binding constants for calicheamicin γ_1^I in restriction fragments and have evaluated their salt dependencies.

Calicheamicin Recognizes a Diverse Class of Sequences. As illustrated in Figure 1A, calicheamicin cleavage in this fragment is primarily directed to three tetranucleotide sequences: the TTGT, ATCT, and TCCT sequences. Inspection of the cleavage distribution in Figure 1 suggests that, at the overlapping TTGT and ATCT sites, two molecules of calicheamicin are bound adjacently with the carbohydrate tail moieties abutting each other, presenting a tail−tail orientation. The three major sites occur within a 25 base pair region of the fragment, and in particular TTGT and ATCT sites are flanked by other weakly cleaved CATT and TTTC secondary sites. Together, these sites form a cluster in this AT-rich region of the fragment. Earlier, Walker et al. (1992), as well as Mah et al. (1994a), identified TTGT as a weak cleavage site compared to the primary TTTT site in their mapping analyses. However, in our pBR322 fragment, cleavage at TTGT is comparable to that at the TCCT site. These results suggest that calicheamicin-mediated binding/cleavage events are greatly influenced by neighboring sequence composition (Zein et al., 1988). *On the basis of mapping analysis in this work, it may be concluded that while sequences of the type TCCT and TTTT are primary cleavage sites, as previously observed, cleavage at other mixed pyrimidine sequences, such as TTGT, varies greatly depending on near neighbor sequences.* It is entirely possible that calicheamicin interaction with one sequence facilitates (or diminishes) the binding/cleavage event at a neighboring sequence.

Site-Specific Calicheamicin Interaction Does Not Involve Counterion Release from DNA. As seen in Figures 4 and 5, there is a sharp difference in the free energy of association at the TCCT site from −8.9 to −7.4 kcal mol^{-1} between 125 and 150 mM NaCl. The site-specific binding constant that we determine at low-salt reaction conditions is higher by 1 order of magnitude than those determined at high-salt reaction conditions. The tighter association under low-salt conditions is consistent with the previously reported binding constant estimation for a TCCT site by Crothers and co-workers (Drak et al., 1991). Their estimation of K_{as} of 3.3 $\times$ 10^7 to 1 $\times$ 10^8 M^{-1} is comparable to our present estimate of 1 $\times$ 10^7 M^{-1} (−8.9 kcal mol^{-1}) for the TCCT site determined at 125 mM NaCl and below. The salt dependence of association constants reported here can explain the discrepancy in binding constants between those obtained by Drak et al. (1991) and those obtained by Ding and Ellestad (1991). The original experiments (Ding & Ellestad, 1991) were carried out in the presence of 100 mM NaCl, whereas the Drak et al. estimates were obtained in the absence of NaCl. More recently, Nicolaou and co-workers used a kinetic analysis of calicheamicin γ_1^I-mediated DNA cleavage to measure the binding affinity to the TCCT site in a 20-mer (Li et al., 1994). Their estimate of 7.4 $\times$ 10^6 M^{-1} in the presence of 20 mM NaCl is in good agreement with our results with a 142 base pair restriction fragment under low-salt conditions.

A theoretical basis for interpreting the effect of ionic strength on DNA−ligand interactions was developed by Manning and Record, who demonstrated that a plot of log K_{obs} versus ln [MX] gives a straight line with a slope of $-Z\psi$, if no other processes are linked to the DNA binding equilibrium. Alternatively, a plot of ΔG_{obs} as a function of ln [MX] yields a slope of $Z\psi RT$ (Record et al., 1991). Z is equivalent to the number of counterions released during drug binding, and ψ is 0.88, which is the fractional neutralization of a phosphate due to condensed counterion. This relationship was used to relate cationic ligand binding to proteins and DNA (Record et al., 1978; Wilson & Tanious 1994).

The salt-dependent free energy of calicheamicin−DNA binding is inconsistent with this relationship, suggesting that counterion release is not a major driving force in the energetics of the complexation. The sharp transition in the salt dependence of the TCCT site is somewhat unusual, especially in view of the fact that ATCT and TTGT binding isotherms are not altered under identical salt conditions. It is possible that the observed salt-dependent free energy differences in the TCCT site are due to coupling of the calicheamicin−DNA binding equilibrium to salt-dependent DNA conformational changes. The DNA cleavage reactions were carried out in a medium consisting of salt and ethanol, conditions that are likely to facilitate overwinding of the helix and dehydration of the minor groove (Chan et al., 1979; Baase & Johnson, 1979; Anderson & Bauer, 1978) in the presence of calicheamicin. Therefore, in high salt, calicheamicin conceivably binds to a slightly more dehydrated DNA structure with a *lower apparent binding free energy*. Decreased hydration of the DNA minor groove matrix could result in a diminished entropic contribution to binding (Tanious et al., 1992). Consistent with this is the earlier temperature-dependent binding studies that suggested a significant entropic contribution with a large negative heat capacity change, due to water release in the formation of the calicheamicin−DNA complex (Ding & Ellestad, 1991). Earlier, Suguira and co-workers reported that esperamicin−DNA association is also facilitated by entropic contributions due to water release from DNA (Uesugi & Suguira, 1993).

Aside from the salt-dependent transition between 125 and 150 mM NaCl for the TCCT site, there is no observable salt dependence of calicheamicin binding to these sequences between 50 and 125 mM NaCl and between 150 mM and 1 M NaCl. The slope of the log−log plot of free energy versus NaCl is not linear and therefore produced poor linear fits to the Record equation (Record et al., 1991), suggesting that there is no counterion release from the DNA−calicheamicin association. However, DNA interactions of many other cationic small molecules, such as netropsin and related analogues (Lee et al., 1989) irehdiamine (Marky et al., 1983a) and daunomycin (Marky et al., 1983b; Chaires, 1985), are stabilized by ion interactions between the positively charged amine group and the negatively charged DNA with concomitant release of sodium ions (Wilson & Tanious 1994). Unlike these other ligands, calicheamicin consists of a secondary amine with bulky deoxy sugar and alkyl group substituents. Furthermore, the ethylamino sugar (E ring) in calicheamicin is part of a relatively rigid molecule (Walker et al., 1990) and probably binds externally to the polyphosphate backbone. Therefore, the diminished importance of electrostatic interactions in this instance may be due to (i) restricted rotation that would otherwise have provided optimal ionic contact with the DNA polyphosphate backbone, as well as to (ii) positioning of the amino sugar external to the minor groove. Our observations, however, do not exclude the role of the ethylamino group in nonspecific electrostatic association with the DNA and as a hydrogen bond donor along the DNA phosphate backbone. A salt bridge between the positively charged nitrogen of the

ethylamino group and a phosphate moiety has been proposed by both Kahne and Nicolaou and their co-workers. However, their NMR studies did not provide direct evidence for such an interaction (Walker et al., 1993; Paloma et al., 1994).

CONCLUSIONS

A quantitative DNA cleavage method has been used to measure the equilibrium binding constants for calicheamicin interactions with recognition sites within a DNA restriction fragment as a function of salt concentration at 0 and 23 °C and at pH 7.5 and 8.1. In this restriction fragment, the high-affinity recognition sites are the TTGT, ATCT, and TCCT sequence tetramers. The free energy of the TCCT−calicheamicin complex formed at low salt (<150 mM) is increased by ~1 kcal relative to the free energy at high salt (150 mM and above). The free energy of calicheamicin interactions with TTGT and ATCT sequence tetramers is however, independent of salt. All three free energy data sets suggest that the electrostatic forces between the positively charged E ring ethylamino group and the negatively charged phosphate backbone (Walker et al., 1993) are not major determinants in the overall binding energetics. These results further suggest that nonionic forces rather than electrostatic interactions stabilize specific DNA−calicheamicin interactions. The overriding importance of these forces is possibly due to several structural aspects of the amino group, including orientation of charge, shielding/steric effects, and the presence of large hydrophobic substituents.

REFERENCES

Ackers, G. K., Shea, M. A., & Smith, F. R. (1983) *J. Mol. Biol. 170*, 223−242.

Anderson, P., & Bauer, W. (1978) *Biochemistry 17*, 594−600.

Baase, W. A., & Johnson, W. C. (1979) *Nucleic Acids Res 6*, 797−814.

Brenowitz, M., Senear, D. F., Shea, M. A., & Ackers, G. K. (1986a) *Methods Enzymol. 130*, 132−181.

Brenowitz, M., Senear, D. F., Shea, M. A., & Ackers, G. K. (1986b) *Proc. Natl. Acad. Sci. U.S.A. 83*, 8462−8466.

Chaires, J. B. (1983) *Biochemistry 22*, 4202−4211.

Chaires, J. B., Dattagupta, N., & Crothers, D. M. (1982) *Biochemistry 21*, 3933−3940.

Chan, A., Kilkuskie, R., & Hanlon, S. (1979) *Biochemistry 18*, 84−91.

Chatterjee, M., Cramer, K. D., & Townsend, C. A. (1993) *J. Am. Chem. Soc. 115*, 3374−3375.

Colocci, N., Distefano, M. D., & Dervan, P. B. (1993) *J. Am. Chem. Soc. 115*, 4468−4473.

Cramer, K. D., & Townsend, C. A. (1991) *Tetrahedron Lett. 32*, 4635−4638.

Dattagupta, N. D., Hogan, M., & Crothers, D. M. (1980) *Biochemistry 19*, 260−267.

Dedon, P. C., Salzberg, A. A., & Xu, J. (1993) *Biochemistry 32*, 3618−3622.

DeVoss, J. J., Townsend, C. A., Ding, W.-d., Morton, G. O., Ellestad, G. A., Zein, N., Tabor, A. B., & Schreiber, S. L. (1990) *J. Am. Chem. Soc. 112*, 9669−9670.

Ding, W.-d., & Ellestad, G. A. (1991) *J. Am. Chem. Soc. 113*, 6617−6620.

Drak, J., Iwasawa, N., Danishefsky, S., & Crothers, D. M. (1991) *Proc. Natl. Acad. Sci. U.S.A. 88*, 7464−7468.

Eftink, M. R., Anusiem, A. C., & Biltonen, R. L. (1983) *Biochemistry 22*, 3884−3896.

Ellestad, G. A., Hamann, P. R., Zein, N., Morton, G. O., Siegel, M. M., Pastel, M., Borders, D. B., & McGahren, W. J. (1989) *Tetrahedron Lett. 30*, 3033−3036.

Golik, J., Clardy, J., Dubay, G., Groenewold, G., Kawaguchi, H., Konishi, M., Krishnan, B., Ohkuma, H., Saitoh, K., & Doyle, T. W. (1987a) *J. Am. Chem. Soc. 109*, 3461−3462.

Golik, J., Dubay, G., Groenewold, G., Kawaguchi, H., Konishi, M., Krishnan, B., Ohkuma, H., Saitoh, K., & Doyle, T. W. (1987b) *J. Am. Chem. Soc. 109*, 3462−3464.

Hangeland, J. J., DeVoss, J. J., Heath, J. A., Townsend, C. A., Ding, W.-d., Ashcroft, J. S., & Ellestad, G. A. (1992) *J. Am. Chem. Soc. 114*, 9200−9202.

Herrara, J. E., & Chaires, J. B. (1989) *Biochemistry 28*, 1993−2000.

Johnson, M. L., & Faunt, L. M. (1992) *Methods Enzymol. 210*, 1−37.

Koblan, K. S., Bain, D., Beckett, D., Shea, M. A., & Ackers, G. K. (1992) *Methods Enzymol. 210*, 405−425.

Krishnamurthy, G., Ding, W.-d., O'Brien, L., & Ellestad, G. A. (1994) *Tetrahedron 50*, 1341−1349.

Lee, M. D., Dunne, T. S., Siegel, M. M., Chang, C. C., Morton, G. O., & Borders, D. B. (1987a) *J. Am. Chem. Soc. 109*, 3464−3466.

Lee, M. D., Dunne, T. S., Chang, C. C., Ellestad, G. A., Siegel, M. M., Morton, G. O., McGahren, W. J., & Borders, D. B. (1987b) *J. Am. Chem. Soc. 109*, 3466−3468.

Lee, M. D., Manning, J. K., Williams, D. R., Kuck, N. A., Testa, R. T., & Borders, D. B. (1989) *J. Antibiot. 42*, 1070−1087.

Lee, M. D., Ellestad, G. A., & Borders, D. B. (1991) *Acc. Chem. Res. 24*, 235−243.

Lee, M. D., Dunne, T. S., Chang, C. C., Siegel, M. M., Morton, G. O., Ellestad, G. A., McGahren, W. J., & Borders, D. B. (1992) *J. Am. Chem. Soc. 114*, 985−997.

Lee, M. D., Durr, F. E., Hinman, L. M., Hamann, P. R., & Ellestad, G. A. (1993) in *Advances in Medicinal Chemistry* (Maryanoff, B. E., & Maryanoff, C. A., Eds.) Vol. 2, pp 31−66, JAI Press Inc., Greenwich, CT.

Li, T., Zeng, Z., Estevez, V., Baldenius, K. U., Nicolaou, K. C., & Joyce, G. F. (1994) *J. Am. Chem. Soc. 116*, 3709−3715.

Mah, S. C., Townsend, C. A., & Tullius, T. C. (1994a) *Biochemistry 33*, 614−621.

Mah, S. C., Price, M. A., Townsend, C. A., & Tullius, T. D. (1994b) *Tetrahedron 50*, 1361−1378.

Marky, L. A., Snyder, J. G., & Breslauer, K. J. (1983) *Nucleic Acids Res. 16*, 5701−5715.

Maxam, A. M., & Gilbert, W. (1980) *Methods Enzymol. 65*, 499−560.

Myers, A. G., Cohen, S. B., & Kwon, B.-m. (1994) *J. Am. Chem. Soc. 116*, 1255−1271.

Paloma, L. G., Smith, J. A., Chazin, W. J., & Nicolaou, K. C. (1994) *J. Am. Chem. Soc. 116*, 3697−3708.

Record, M. T., Jr., Anderson, C. F., & Lohman, T. M. (1978) *Q. Rev. Biophys. 11*, 103−178.

Record, M. T., Jr., Ha, J.-H., & Fisher, M. A. (1991) *Methods Enzymol. 208*, 291−343.

Reiner, P., & Brenowitz, M. (1991) *Comput. Appl. Biosci. 7*, 337−340.

Senear, D. F., & Bolen, D. W. (1992) *Methods Enzymol. 210*, 463−481.

Senear, D. F., Brenowitz, M., Shea, M. A., & Ackers, G. K. (1986) *Biochemistry 25*, 7344−7354.

Singleton, S. F., & Dervan, P. B. (1992a) *J. Am. Chem. Soc. 114*, 6956−6965.

Singleton, S. F., & Dervan, P. B. (1992b) *Biochemistry 31*, 10995−11003.

Tanious, F. A., Veal, J. M., Buczak, H., Ratmeyer, L. S., & Wilson, W. D. (1992) *Biochemistry 31*, 3103−3112.

Uesugi, M., & Suguira, Y. (1993) *Biochemistry 29*, 4622−4627.

Walker, S. L., Valentine, K. G., & Kahne, D. (1990) *J. Am. Chem. Soc. 112*, 6428−6429.

Walker, S. L., Landovitz, R., Ding, W.-d., Ellestad, G. A., & Kahne, D. (1992) *Proc. Natl. Acad. Sci. U.S.A. 89*, 4608−4612.

Walker, S. L., Murnick, J., & Kahne, D. (1993) *J. Am. Chem. Soc. 115*, 7954−7961.

Walker, S. L., Andreotti, A. H., & Kahne, D. E. (1994) *Tetrahedron 50*, 1351−1360.

Wilson, W. D., & Tanious, F. A. (1994) in *Molecular Aspects of Anticancer Drug-DNA Interactions* (Neidle, S., & Waring, M., Eds.) pp 243−269, Vol. 2, MacMillan, London.

Zein, N., Sinha, A. M., McGahren, W. J., & Ellestad, G. A. (1988) *Science 240*, 1198−1201.

Zein, Z., Poncin, M., Nilakantan, R., & Ellestad, G. A. (1989) *Science 244*, 697−699.

BI9412536